Carbohydrate Polymers 234 (2020) 115919

Contents lists available at ScienceDirect

Carbohydrate Polymers

journal homepage: www.elsevier.com/locate/carbpol

Effect of solvent and ions on the structure and dynamics of a hyaluronan molecule

Eva Kutálková[a], Josef Hrnčiřík[a], Roman Witasek[a], Marek Ingr[a,b,*]

[a] Tomas Bata University in Zlín, Faculty of Technology, Department of Physics and Materials Engineering, Nám. T.G. Masaryka 5555, 76001 Zlín, Czech Republic
[b] Charles University, Faculty of Science, Department of Biochemistry, Hlavova 8/2030, 12843 Praha 2, Czech Republic

ARTICLE INFO

Keywords:
Hyaluronan
Random coil
Ions
Solvation shell
Molecular dynamics

ABSTRACT

Hyaluronic acid (hyaluronan, HA) is a negatively charged polysaccharide forming highly swollen random coils in aqueous solutions. Their size decreases along with growing salt concentration, but the mechanism of this phenomenon remains unclear. We carry out molecular-dynamics simulations of a 48-monosaccharide HA oligomer in varying salt concentration and temperature. They identify the interaction points of Na^+ ions with the HA chain and reveal their influence on the HA solvation-shell structure. The salt-dependent variation of the molecular size does not consist in the distribution of the dihedral angles of the glycosidic connections but is driven by the random flips of individual dihedral angles, which cause the formation of temporary hairpin-like structures effectively shortening the chain. They are induced by the frequency of cation-chain interactions that grow with the salt concentration, but is reduced by the simultaneous decrease of ions' activities. This leads to an anomalous random-coil shrinkage at 0.6 M salt concentration.

1. Introduction

Hyaluronan (HA), a natural polysaccharide of the extracellular matrix of connective tissues, is a linear alternating co-polymer of glucuronic acid (GCU) and N-acetyl glucosamine (NAG) of the formula ([4)-β-D-GlcpA-(1→3)-β-D-GlcpNAc-(1→]$_n$). As a highly hydrophilic polyelectrolyte it forms highly swollen random coils in aqueous solutions the shape of which varies with the changes of the environment. Indeed, the variations of the radius of gyration (R_g) of HA macromolecules were studied by several research groups (Fouissac, Milas, Rinaudo, & Borsali, 1992; Hayashi, Tsutsumi, Nakajima, Norisuye, & Teramoto, 1995; Mendichi, Soltés, & Giacometti Schieroni, 2003) showing that the growing salt concentration causes the decrease of R_g and thus the shrinkage of the molecule. Recently, differences in the HA random-coil size in the solutions of different Hofmeister-series ions was investigated (Musilová, Kašpárková, Mráček, Minařík, & Minařík, 2019). In addition, more detailed structural studies based on NMR were carried out aimed at the determination of the detailed 3D structure of the HA molecule and its dynamics in solution, often supplemented by the methods of computational chemistry. This approach was first used by Holmbeck et al. who determined the interglycosidic dihedral angles and predicted the properties of the helical structure of HA oligosaccharides (Holmbeck, Petillo, & Lerner, 1994). Donati et al. showed that the relative rigidity of the HA chain is supported by the formation of direct or water-mediated intramolecular hydrogen bonds (Donati, Magnani, Bonechi, Barbucci, & Rossi, 2001). The dynamics of the chain was studied by Furlan, La Penna, Perico, & Cesàro (2005) and by the group of Blundell who used the ^{13}C- and ^{15}N-labeled oligosaccharides to evaluate the flexibility of both the sidechains and the glycosidic connections (Almond, Deangelis, & Blundell, 2006; Almond, DeAngelis, & Blundell, 2005; Blundell, DeAngelis, Day, & Almond, 2004). These studies also confirmed the left-handed 4-fold helical structure of the HA oligosaccharides previously known from the crystal structures.

Recently, HA oligosaccharides modified by aliphatic chains of different lengths were simulated by MD showing an increasing tendency of formation of particles with hydrophobic core when the chain is growing (Payne, Svechkarev, Kyrychenko, & Mohs, 2018). MD was also used to study interactions of HA oligosaccharides with phospholipids (Bełdowski, Mazurkiewicz, Topoliński, & Małek, 2019; Siódmiak et al., 2017) and biomembranes (Smith, Ziolek, Gazzarrini, Owen, & Lorenz, 2019). Using quantum-chemical methods HA oligosaccharides were studied by Pogány and Kovács (Pogany & Kovacs, 2010) who carried out a DFT study of isolated di- to decasaccharides and determined their hydrogen-bonds structure and its influence on the conformation. For a comprehensive survey of NMR and computational studies see the recent reviews (Almond, 2018; Nagarajan, Sankaranarayanan, & Desai, 2019; Pomin, 2014).

In our previous work we presented a method of calculating the

* Corresponding author.
E-mail addresses: kutalkova@utb.cz (E. Kutálková), hrncirik@utb.cz (J. Hrnčiřík), witasek@utb.cz (R. Witasek), ingr@utb.cz (M. Ingr).

https://doi.org/10.1016/j.carbpol.2020.115919
Received 5 November 2019; Received in revised form 18 January 2020; Accepted 25 January 2020
Available online 27 January 2020

random-coil size from a simulation of a short oligosaccharide (Ingr, Kutálková, & Hrnčiřík, 2017). The values of the radius of gyration obtained this way agreed well with experiment for a wide range of HA molecular weight and for several different values of the salt concentration in the solution. However, the detailed mechanisms by which the dissolved ions influence the size and shape of the random coil remains unclear. No apparent differences in the chain structure under different salt concentration were observed, especially not the changes in dihedral angles of glycosidic connections. Moreover, the common cause of polyelectrolyte-molecule shrinkage in salty solutions – screening of the electrostatic repulsion, seems to be rather insignificant for HA due to the large distances of the charged groups. Hence, in this work we concentrate on the explanation of how the interactions of the HA chain with the solvation shell, especially the ions, are transmitted to the dynamical changes of the chain structure and, subsequently, to the changes of the shape and size of the random coils. The aim of this study is thus to verify the following hypothesis: Ions in solution influence the size and shape of hyaluronan random coils by direct interactions with specific sites on the chain via the dynamic formation and decay of hairpin-like loops.

2. Methods

2.1. Simulation of hyaluronan oligosaccharides

HA oligonucleotides of 48 monosaccharide units (24-mer, as a monomeric units consists of two residues, GCU and NAG) were simulated in 1 M, 0.6 M, 0.2 M and 0 M (polyelectrolyte only neutralized by counterions Na^+) NaCl solution at two different temperatures (275 K, 310 K). The initial dimensions of the water box were (177 × 103 × 172) $Å^3$. Topology files were constructed using a NAMD automatic PSF builder, solvent molecules were represented by the explicit TIP3P solvent model, periodic boundary conditions in the isobaric-isothermal (NPT) ensemble were used. All simulations were performed using NAMD Version 2.10 program package (Phillips et al., 2005) with CHARMM36 carbohydrate topology and force field parameters (Guvench, Hatcher, Venable, Pastor, & MacKerell, 2009; Guvench et al., 2008) which is one of the standard ways used for carbohydrate simulations (Nagarajan et al., 2019). A timestep of 1 fs for bonding and 2 fs for non-bonded interactions and 10 Å cutoff of non-bonded interactions were used. Full electrostatic calculations were performed every sixth fs using the Particle Mesh Ewald method (PME), implemented in the NAMD package. Prior to each MD simulation the energy of systems was minimized for 180 fs. Subsequent simulations were carried out at the constant atmospheric pressure and one of the temperatures mentioned. The pressure was controlled using the Langevin piston Nosé-Hoover method and the temperature was controlled using Langevin dynamics. Interatomic distances and non-bonded interactions were evaluated using VMD 1.9.2 program (Humphrey, Dalke, & Schulten, 1996). In order to reach the thermodynamic equilibrium of the system, the simulation times were between 80 and 100 ns for systems at 310 K temperature about 200 ns for systems at 275 K temperature.

2.2. Cumulative solvation-shell diagrams (CSSD)

CSSD show the projection of all atoms within a certain shape around a given residue to a selected plane. The diagram is a superposition of these projections over a selected number of residues of a given kind (GCU or NAG) and time frames. It is a useful tool to investigate the distribution of individual components of the HA solvation shell. For more details see SI Methods, section SM1.

2.3. Distribution functions of solvent molecules

Distribution functions of solvent molecules show the numbers of atoms of a given kind along a selected axis in one of the three possible directions summed over the two other coordinates. They are summed over selected residues of a given kind and selected time frames and can be limited to a special part of the space. For more details see SI Methods, section SM2.

2.4. Composition of random coils as a function of dihedral-angle distributions

Composition of random coils as a function of dihedral-angle distributions was carried out using the subsequent connecting of individual residues in accord with the distributions of the dihedral angles of the glycosidic connections obtained from the simulation of a certain system. For more details see SI Methods, section SM3.

3. Results and discussion

3.1. End-to-end distance and persistence length of the HA chain

Previously (Ingr et al., 2017), we proposed a method for calculating the radii of gyration of HA composing a long random coil from fragments of a short oligosaccharide. In that calculation the dihedral angles of the glycosidic connections were inherently present in the chain fragments. For the glycosidic bond connecting two fragments the couple of dihedral angles was chosen on random in accord with the distribution of these angles in the ensemble formed by all the glycosidic connections in all the time frames of the simulation. In this work we investigate the mechanism by which the ions of the electrolyte influence the random coil size. MD simulations of HA oligomer of 48 monosaccharide units were carried out for eight systems varying in temperature and NaCl concentration. The mean distances of residue couples separated by different numbers of monomeric units were evaluated. For every separation the distance was averaged over all possible couples throughout the chain length and the selected number of time frames. Fig. 1 shows that for both the temperatures the end-to-end distance of a given separation is the highest for 0 M NaCl. For 310 K this distance decreases continuously along with the growing salt concentration, as expected from the published results (see e.g. Fig. 1B). For the lower temperature, 275 K, the distance decreases up to the concentration of 0.6 M NaCl but above this value it shows an opposite trend.

Given the curves in Fig. 1A, the persistence length of the chain can be calculated for every studied system numerically solving the formula (Kratky & Porod, 1949)

$$\langle d^2 \rangle = 2 l_p L \left[1 - \frac{l_p}{L} \left(1 - e^{-\frac{L}{l_p}} \right) \right], \tag{1}$$

where d is the end-to-end distance, L the contour length and l_p the persistence length. As can be seen from the lower limit of these curves, the contour length per residue is approximately 4.6 Å. The persistence lengths are shown in Fig. 1B (see the legend) together with the dependencies of radii of gyration on molecular weight for systems of given persistence lengths determined by the equation (Benoit & Doty, 1953)

$$\langle R_g^2 \rangle = l_p \left\{ \frac{L}{3} - l_p + \frac{2 l_p^2}{L^2} \left[L - l_p \left(1 - \exp\left(-\frac{L}{l_p} \right) \right) \right] \right\}. \tag{2}$$

Direct comparison of the calculated persistence lengths with experiment can be done for 0 M NaCl – the two experimental values obtained by two different methods at 298 K, 159 Å and 184 Å (Buhler & Boué, 2004), show a good agreement with our results. Furthermore, Fig. 1B shows a good agreement of the calculated R_g values with experiment and indicates that the properties of the simulated oligosaccharide are kept even by a long random coil. Obviously, the flexibility of the chain is strongly influenced by the ions, but the question

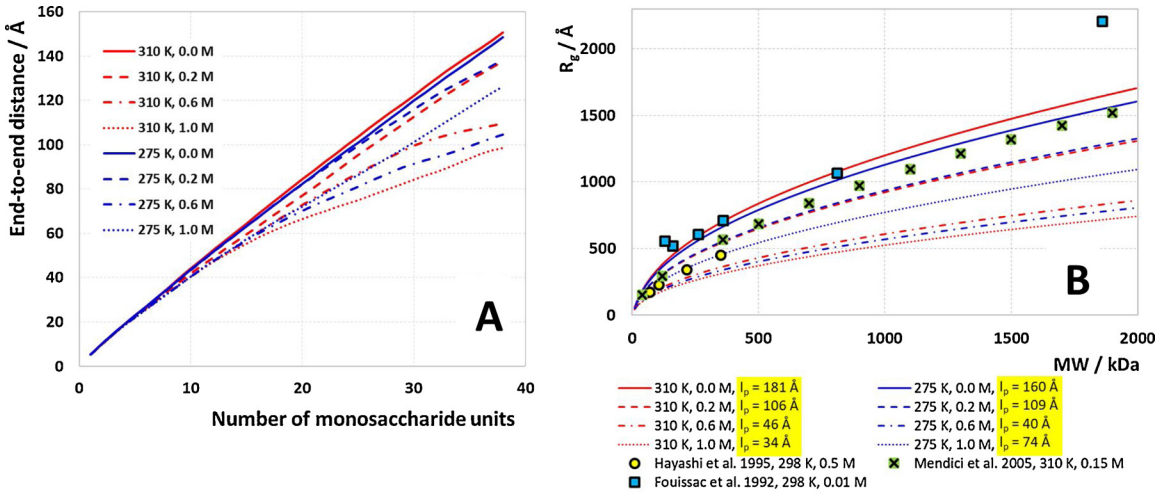

Fig. 1. A. End-to-end distance as a function of the number of monosaccharide units of the oligosaccharide for different temperatures and NaCl concentrations. Every point of each curve is given by the average distance of all possible oligosaccharides of the given length contained in the simulated chain. B. Theoretical dependencies of the radius of gyration on the molecular weight of the HA chain for different conditions (line design corresponds with panel A). R_g was calculated (using eq. 2) from the persistence length of every system (yellow emphasis in the legend) determined by the numerical solution of eq. 1. Selected experimental data are shown for comparison. (For interpretation of the references to colour in this figure legend, the reader is referred to the web version of this article).

remains by what mechanism they effect the structure and shape of the random coil.

3.2. Distribution of dihedral angles of the glycosidic connections

Every two HA residues are connected by a glycosidic bond characterized by two dihedral angles (defined in Fig. S2). As there are two types of glycosidic connection – 1–3 connection of the reducing end of GCU and non-reducing end of NAG and 1–4 connection for the opposite variant– four dihedral angles have to be considered in order to characterize the HA chain. Obviously, when fixed values of the dihedral angles are taken into account, the resulting chain adopts a shape of a regular helix the diameter and ascent of which depend on the choice of the dihedral values. When the distribution is broadened, the regular helix changes to a random coil and its radius of gyration decreases with the width of the distribution. The distribution of individual dihedral angles is shown in Fig. S4, which indicates that the widths of the major peaks are practically independent of the temperature and salt concentration. When an ensemble of random coils of a certain number of monosaccharide units is generated combining individual residues with the dihedral angles of their glycosidic connection obeying the distribution given solely by the major peaks, the radius of gyration is in a good agreement with the values for the salt-free solution of HA from our previous calculation (Ingr et al., 2017) as well as the experiment (Fig. S3). Mutual orientations of the neighboring residues vary only very slightly from the conformation plotted in Fig. 2A, hereafter referred to as “standard conformation”.

A typical appearance of a longer HA molecule is shown in Fig. 3, first panel. Thus, this simple model corresponds with a real system not disturbed by the dissolved ions and shows that at these conditions no additional flexibility of the chain has to be taken into account. In addition, it also proves that the simulation provides a good approximation of the real system.

As the salt concentration increases, minor peaks can be observed in the dihedral-angles distribution which correspond with the flipped glycosidic connections, i.e. connections containing at least one dihedral angle of a value out of the peak corresponding with the standard conformation (see Fig. S4).

If these peaks are added to the dihedrals distribution, the radius of gyration decreases immediately, but the correspondence with experiment is not good – the calculated radii of gyration are generally underestimated (e.g. the R_g value for 0.2 M NaCl, 310 K and 2000 monosaccharide units, i.e. 378 kDa, is 465 Å, which is significantly lower than expected – see the experiments in Fig. 1B). On one hand, this observation indicates that the increased chain flexibility leads to a

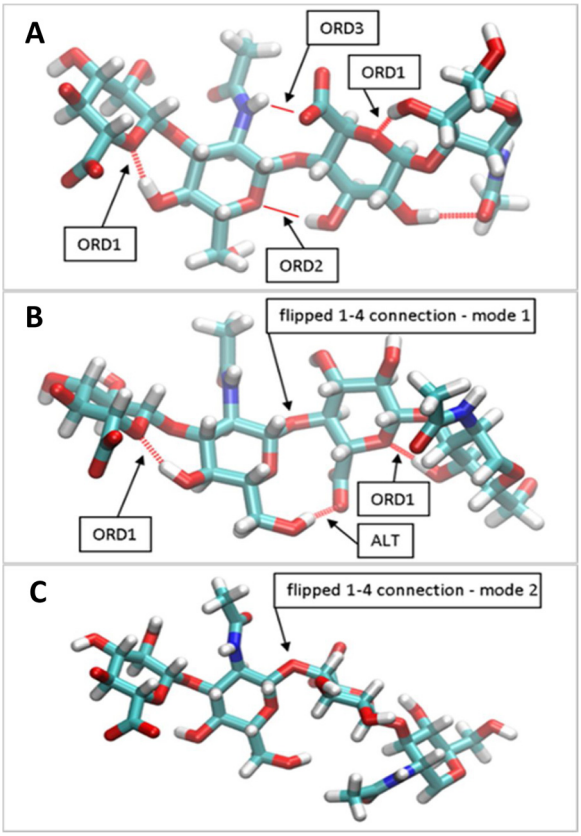

Fig. 2. Conformations of the HA chain. A. Standard conformation of both the 1–3 (left) and 1–4 (right) glycosidic connections of the monosaccharide units with all four dihedral angles in their most typical values. Ordinary hydrogen bonds are depicted by the red lines. B. The most common flipped conformation (mode 1) with the 14_2 dihedral turned to -5°. C. Another flipped conformation with the (mode 2) 14_2 dihedral turned to 42°. (For interpretation of the references to colour in this figure legend, the reader is referred to the web version of this article).

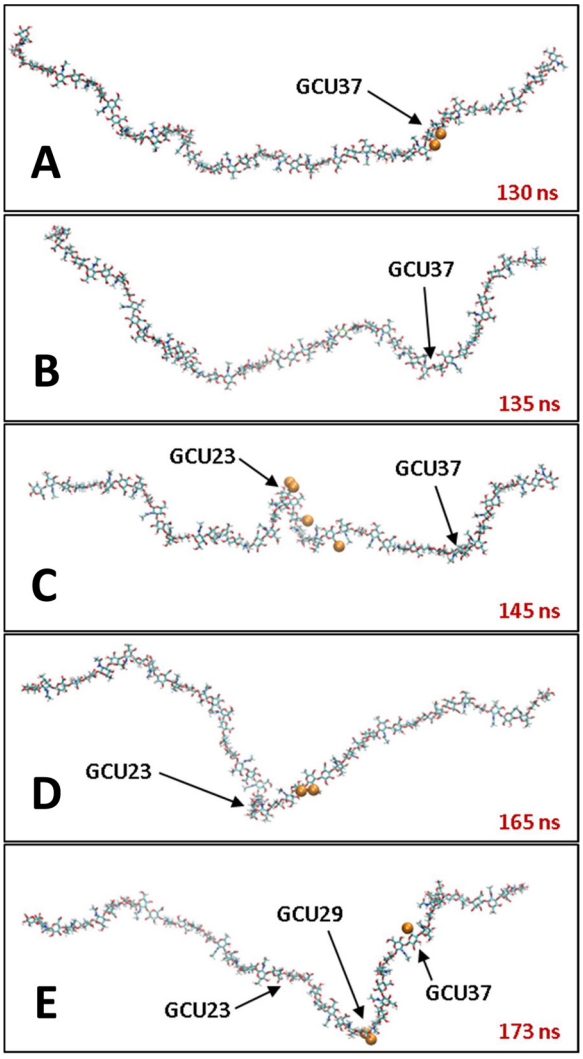

Fig. 3. The development of the HA chain in 1 M NaCl at 275 K during the time course of the simulation. Individual time frames show the rise and vanishing of three hairpin-like structures formed as a consequence of the flip of the 14_2 dihedral angle on the non-reducing end of the GCU units 37, 23 and 29. These structures arise after the disturbance of the standard conformation of the chain by Na^+ (orange balls). The lifetime of these structures is about 10 – 20 ns.

shrinkage of random coils, but, on the other hand, the influence of the minor peaks seems to be exaggerated. The reason is that, due to the hydrodynamic friction, the rest of the molecule remains almost unchanged immediately after the dihedral flip and only slowly relaxes to the new equilibrium conformation enforced by the flip (for detailed discussion see section 3.3.). On the contrary, the model random coil composed of individual residues by the purely statistical approach takes an unnatural turning whenever a dihedral angle from the minor peak is incorporated into the chain as if the equilibrium conformation after the flip was adopted immediately. This strongly increases the disorder of the coil and thus reduces its radius of gyration. Hence, the random incorporation of the dihedral flips into the chain model does not explain the dependence of the radius of gyration on the salt concentration.

3.3. Chain dynamics

Explanation of the chain-dimension variations can be based on the dynamical changes of the chain resulting from the flips of individual dihedral angles of the glycosidic connections. First of all, Fig. 2B and C shows that an individual flip occurs typically at a single glycosidic-

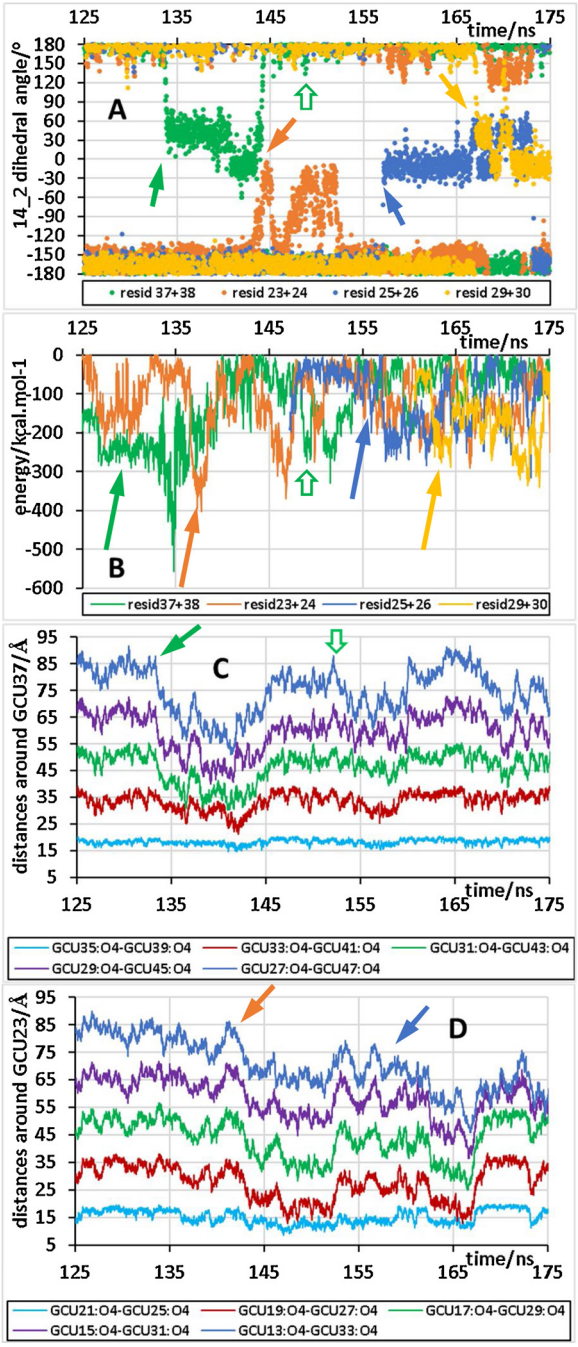

Fig. 4. Time course of the simulation of HA at 1 M NaCl at 275 K. A. Four individual 14_2 dihedral angles between the residues denoted in the legend as functions of time. B. Interaction energy of the residues surrounding the flipping dihedral with Na^+ ions – negative energy indicates Na^+ in the proximity of the residues. C and D. The distances of the residue couples (indicated in the legend) located symmetrically on both sides of the flipping glycosidic connection (indicated in the graph) with growing distance separating them. Note that the flips cause the shortening of the measured distances – formation of hairpin-like structures. The arrows of a given color indicate the related processes in different panels – the residue flip in A, the preceding Na^+-HA interaction in B and the onset of the shortening of the distances between the surrounding residues in C and D. This effect can be, in a lesser extent, caused also by the occurrence of a Na^+ ion close to the respective residues eliciting only a small deviation from the standard dihedral value instead of the complete flip (see the green curves in panels A and B and all curves in panel C from 145 ns on, indicated by the hollow green arrows). Note also that the curves in panel C reflects also the flips at the residues 25 as it is close to residue 23 (the center of measurement in this graph). (For interpretation of the references to colour in this figure legend, the reader is referred to the web version of this article).

connection dihedral angle and no other compensation flips occur anywhere in the chain. With the exception of the flipped dihedral angle, all the geometric parameters are practically equal to the state before the flip. This can be seen comparing Fig. 2A and B, where the connecting dihedral angles are obviously different, but the conformation of the surrounding chains is conserved to such details that e.g. the intramolecular hydrogen bond ORD1 remains unchanged. Therefore, since Fig. 4A shows that the flip itself is a rapid process, in the first moment after its occurrence the chain gets twisted as a ribbon held firmly on one end and turned around its axis on the other end. Moreover, the flip elicits a tendency of the chain to a bending given by the new orientation of the residues neighboring with the flip that assume different directions of each side of the chain compared to the unperturbed chain. Subsequently, the tension in the chain starts to relax and the chain undergoes bending in the point of the flipped connection, therefore the residues on the different sides of this connection get closer to one another and form a loose hairpin-like loop until the chain conformation reaches a new equilibrium.

As the flipped conformation is a thermodynamically unfavorable state, after a certain time period it undergoes a reverse flip that generates oppositely oriented tension and results in the reverse relaxation to the original chain conformation followed by the growth of the distance between the residues on the opposite sides of the flip. The time dependence of the separating distance of several such residue couples is shown in Fig. 4C and D. Every formation of the hairpin-like loop is preceded by a local interaction of Na^+ ions with the respective spot of the chain. Fig. 4B documents these interactions as a decrease of the HA-Na^+ interaction energy. It indicates the key role of these interactions for the formation of the loops (the mechanism is described in detail in section 3.4.2.). Fig. 3 in section 3.2. documents the subsequent formation of several hairpin-like loops during the course of the simulation. Fig. 3A shows the initial interaction of the chain at GCU37 with the Na^+ ions while Fig. 3B shows the formed loop around this residue which later decays at Fig. 3C. This process is also shown in detail in Fig. S5 which indicates that the formation of the hairpin-like loop culminates at 138 ns. Fig. 3C also shows the loop formed around GCU23 with the Na^+ ions still present. In Fig. 3D it is already decayed but other Na^+ ions are present close to GCU29. These ions initiate the formation of a loop around this residue as can be seen in Fig. 3E. Figs. 3 and S5 show that an average lifetime of the loop is in lower tens of ns. In the HA chain the most often flip occurs on the 1–4 connection, especially the dihedral 14_2. The standard mean value of this dihedral is about –171° and there are two main extraordinary values, –5° and 42°. As can be seen in Fig. 4A, the flipped dihedral often jumps between these two values and the jump from one to another may lead to even deeper decrease of the distance between the surrounding residues. Obviously, the repeated process of a formation and decay of the loops leads to the shortening of the mean end-to-end distance and radius of gyration of the molecule. The described process is thus the cause of the variations in the random-coil size of the HA macromolecule in different environments which support the formation of the hairpin-like loops with different intensity.

3.4. Solvent effects on the chain dynamics

The frequency of the dihedral flips is approximately proportional to the NaCl concentration (see the secondary peaks in Fig. S4). The effect of the ions can be mediated either by the influence of the ions on its solvation shell including the formation of hydrogen bonds or by a direct interaction of an ion with the oligosaccharide.

3.4.1. Hydrogen bonds formation

Hyaluronan chain contains various functional groups serving as both donors and acceptors of hydrogen bonds. Therefore, a peculiar network of these bonds is formed within the molecule and many others interconnect the HA molecule and the surrounding solvent. A generally

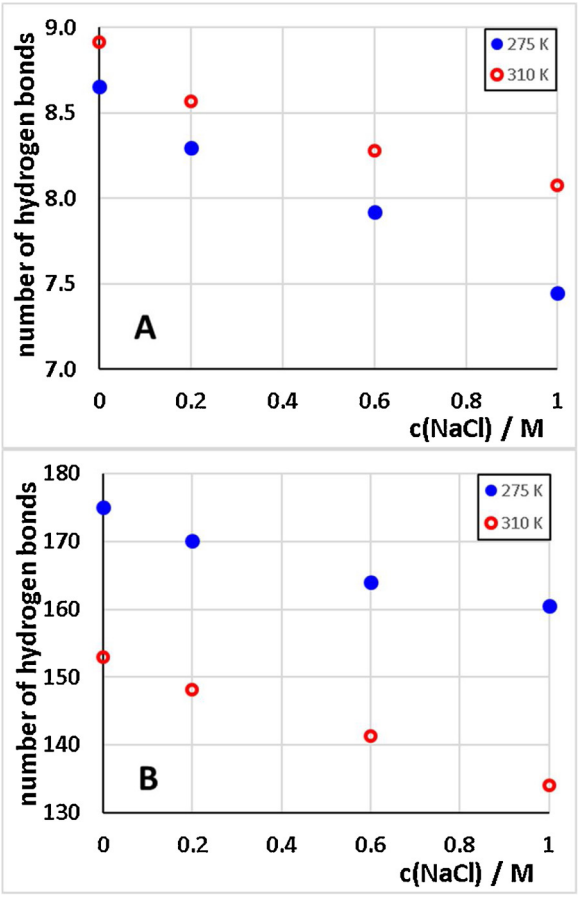

Fig. 5. Numbers of ordinary hydrogen bonds (A) within the simulated HA chain and HA-water hydrogen bonds (B). The error bars smaller than the used symbols.

accepted concept describes three main hydrogen bonds within the HA chain which stabilize the ordinary structure of the macromolecule (Fig. 2A, hereafter called “ordinary hydrogen bonds”). These hydrogen bonds are formed by 1. O4 (NAG) – O5 (GCU), 2. O3 (GCU) – O5 (NAG) and 3. N (NAG) – O61 (donor group is written first; for identification of the atom see Fig. S1). The hydrogen bond 1 bridges the 1–3 connection while the hydrogen bonds 2 and 3 bridge the connection 1–4. In addition, several different hydrogen bonds (hereafter called “alternative hydrogen bonds”) can be formed occasionally that are capable of a temporary stabilization of different extraordinary structures occurring especially as a consequence of the dihedral-angle flips (e.g. “ALT” in Fig. 2B). Using equilibrium MD simulations we have evaluated the average numbers of hydrogen bonds within the last 36 ns of the simulation at two different temperatures and several different NaCl concentrations. Fig. 5 shows that the total number of intramolecular hydrogen bonds within the simulated HA oligosaccharide increases along with the temperature.

On the contrary, the number of hydrogen bonds between the molecule and the solvent shows an opposite trend. Both these hydrogen bonds likely contribute to the straightening of the HA chain, the intramolecular ones by fixing the standard conformation and the HA-water ones by forcing the oligosaccharide to expose the oxygen containing groups to water. These effects are thus counteracting, but the relative decrease of the HA-water hydrogen bonds is higher than the increase of the intramolecular ones (compare the numbers given in the two panels of Fig. 5). Temperature increase may therefore rather destabilize the standard conformation. However, in pure water this effect is negligible, but may contribute to the observed conformation changes in the presence of ions. When the salt concentration is increased, the

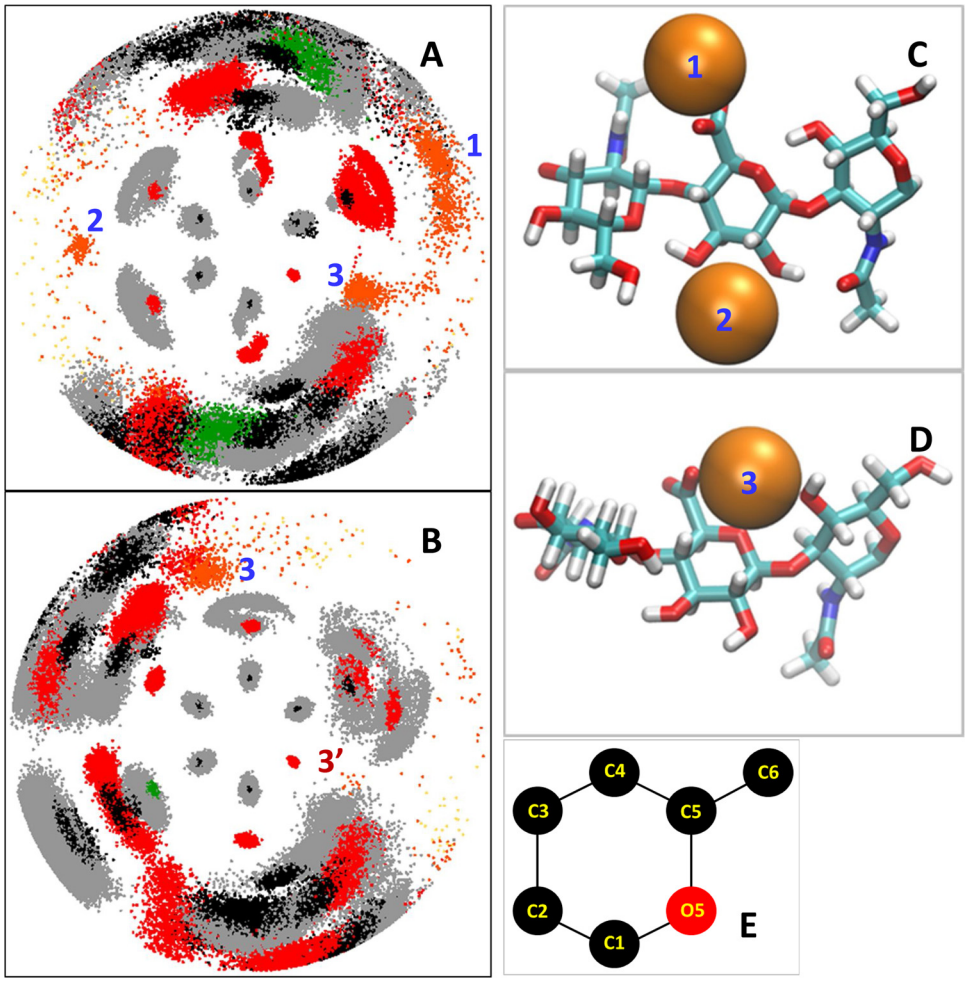

Fig. 6. A and B. Cumulative solvation-shell diagrams of the GCU and NAG residues, respectively. The monosaccharide ring is viewed in the direction of its 3-fold "axis of symmetry". Carbon atoms are shown in black, oxygen in red, hydrogen in grey, nitrogen in green, Na^+ in orange and Cl– in yellow. Atoms of water are not shown. The three typical locations of Na^+ are indicated: 1. at the carboxylate group of GCU, 2. between the oxygens O2 and O3 of GCU, 3. in the proximity of the oxygen O5 of GCU (labeled also in the NAG diagram). With NAG the Na^+ ions interact weakly in a position analogous to 3 – labeled as 3′. C. Structure of a HA chain with two Na^+ ions in positions 1 and 2. D. Structure of a HA chain with a Na^+ ion in the position 3. E. Orientation scheme for CSSDs. For more detailed analysis of CSSDs see Figs. S6-S8. (For interpretation of the references to colour in this figure legend, the reader is referred to the web version of this article).

number of hydrogen bonds of any kind decreases at both the temperatures. Hence, the increasing salt concentration may weaken the highly swollen standard configuration by lowering the hydrogen-bond number and thus further support the dynamic phenomena of loop formations (see section 3.3.) by the increased flexibility of the chain.

3.4.2. HA-ions interactions

The solvation shell of a HA molecule was studied using the cumulative solvation-shell diagrams showing the superposition of atoms around individual residue types in a given direction of view and a selected part of the space over the whole simulation run (see section 2.2.) and the distribution functions of individual atoms of the solvent molecules (see section 2.3.). Especially the distribution of ions around the HA chain was of a special interest. Fig. 6 shows specific positions in which Na^+ ions are often located. The most frequent position of these ions is in the close proximity of the carboxylate group (position 1).

Another position of Na^+ location is between the oxygens 2 and 3 of the GCU unit where the ion is stabilized by the partial charges of these oxygens (position 2). The position 3 is in the proximity of the hemiacetal oxygen O5 of the GCU residue. Here, the ion is attracted by the partial negative charges on this oxygen as well as the oxygen on C6 of the NAG residue and the oxygens of the carboxylate group. The analogous position on the NAG residue (denoted as 3′) is also occasionally occupied by the Na^+ ions, but this event is much less frequent than on GCU (compare the number of dots in these positions in Fig. 6A and B as well as in the corresponding panels of Figs. S7 and S8). If the ion gets in this position, the two participating residues turn out of the standard conformation and impose some tension to the neighboring glycosidic connections. Moreover, the ionic interaction competes with the hydrogen bond (ordinary hydrogen bond ORD1, Fig. 2) formation, which further destabilizes the standard conformation. As a result, the occurrence of Na^+ in this position often induces an orientation flip of the neighboring glycosidic connection, especially the closest 14_2 dihedral angle, as shown in Fig. 2. This phenomenon can be directly observed in the simulations and is also documented by the graph in Fig. 4 which shows the interaction energy between the ion and the participating residues simultaneously with the value of the flipped dihedral angle. Obviously, the increased interaction is well correlated with the dihedral flip. As can be seen in Fig. 4, not only the flip, but, with lower intensity, even the occurrence of a Na^+ ion in the respective position itself leads to the formation of the hairpin-like structures discussed in section 3.3. and therefore to the shortening of the end-to-end distance. Thus, the presence of Na^+ in the position 3 induces the orientation flips of the neighboring residues, which is likely the essence of the mechanism by which the ions influence the random-coil structure.

An ion residing at the proximity of a GCU residue often fluctuates between the positions at the carboxylate group and at O5. In most cases the equilibrium between these two states is shifted towards the carboxylate group, i.e. the ion spends more time in this position than in the other one. However, at the NaCl concentration of 0.6 M the equilibrium seems to be shifted towards the position at O5, which is apparent especially at the lower temperature of 275 K. Figs. S7 and S9 show the distributions of Na^+ ions in these two positions and Fig. 7 the equilibrium ratio of these two states

$$K = \frac{n_{fr}(pos.\ 3)}{n_{fr}(pos.\ 1)}, \tag{3}$$

where n_{fr} denotes the numbers of events when an ion resides in the

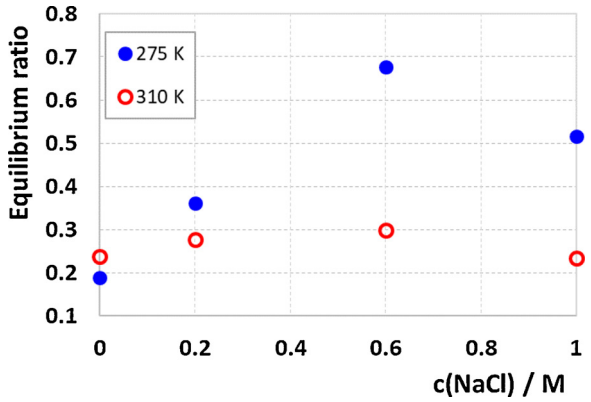

Fig. 7. Equilibrium ratio of ion binding to position 3 (at oxygen O5) vs. position 1 (at carboxylate group) as a function of NaCl concentration. Only the values for non-zero concentrations are derived from the simulation, the values for c (NaCl) = 0 is obtained by extrapolation.

respective position in a given time frame of the simulation.

Fig. S10 shows the total time spent by the ions in position 3 and the mean lifetime spent there during one event of ion binding to this position. Data of all these plots correlate with the reversed order of the end-to-end distances for different NaCl concentrations including the anomaly at 275 K, where the distance for 0.6 M is apparently lower than for 1.0 M. Similar reversed salt influence at a given concentration, known as the Hofmeister series reversal, was observed experimentally for various molecules and biomolecules (Jordan, Gibb, Wishard, Pham, & Gibb, 2018; Salis, Cugia, Parsons, Ninham, & Monduzzi, 2012; Zhang & Cremer, 2009). This behavior may be a consequence of two counteracting quantities – the growing NaCl concentration and the decreasing activity of the ions (Hamer & Wu, 1972) and charged groups along with it. Hence, the ability of constituting the carboxylate-Na^+ couples is likely the lowest at the NaCl concentration close to 0.6 M which results in a prolonged lifetime of the ion at O5 and an increased probability of the dihedral flip leading to the shortening of the end-to-end distance. As this shortening correlates with the occurrence of Na^+ in the position 3, the anomalous behavior even further supports the hypothesis of the key of the HA-Na^+ interaction in this position as the triggering agent of the dynamic changes leading to the random-coil shrinkage.

In summary, the increased NaCl concentration affects the conformation of a HA molecule in two ways, both of which lead to the disruption of the standard conformation. First, the number of hydrogen bonds between HA and water decreases which disturbs the standard conformation by the destabilization of the solvation shell of the molecule. Second, the increased number of Na^+ ions causes their more frequent occurrence in the proximity of charged and polar groups of the HA chain, especially at the proximity of the O5 oxygen (of GCU, but in a lesser extent also for NAG) that plays a key role in the formation of the temporary hairpin-like loops that are essential for the fluctuations of the macromolecular dimensions.

4. Conclusions

A hyaluronan macromolecule is a highly dynamic system the structure of which reflects the surrounding environment. In pure water the chain is more rigid which leads to larger, i.e. more swollen random coils, while in the growing concentration of NaCl the size of the coil shrinks. However, the major peaks of the distributions of the four dihedral angles of both the glycosidic connections of the alternating monosaccharide units show negligible changes in the varying salt concentration and the random coils composed in accord with them are close to the experimental values for HA in pure water irrespective of the salt concentration in the simulated system. The coil-size variations thus do not consist in the differences of the dihedrals distributions, but rather in the structural fluctuations caused by the occasional temporary flips of individual dihedral angles to different orientations or at least partial deflections from the standard orientation. These flips are correlated with the presence of ions, especially Na^+, which interact with the chain in several specific positions but have also an indirect influence on the solvation sphere of the molecule resulting in a lower number of hydrogen bonds. The flip occurs in just one glycosidic connection of the residues and thus brings considerable tension to the chain. Subsequent relaxation of this tension provokes structural changes leading to hairpin-like loops. Their presence in the chain shortens its end-to-end distance as well as the radius of gyration. The lifetime of the flips is in the orders of units to tens of ns after which the glycosidic connection returns to the standard orientation and the hairpin-like loop relaxes to the standard, i.e. straightened, chain conformation. Hence, although these structural variations appear and disappear dynamically, their presence in the chain makes the random coil more compact. The trend of random-coil shrinkage with the growing salt concentration shows an anomaly at the concentration of 0.6 M where the size of the coil is below the general trend, which is especially evident at low temperature. This is likely caused by the lowered occurrence of the Na^+ in the proximity of the carboxylate group that might be a consequence of the optimum combination of the growing salt concentration and the simultaneous decrease of activities of both the charged entities. This destabilizes the interaction between the carboxylate group and the Na^+ ion which has therefore a higher tendency to interact with the HA chain in the proximity of the oxygen O5 where it can provoke the conformation changes.

Although the presented approach is able to reproduce the experimentally observed characteristics of the HA chain and to give a plausible explanation of its behavior, it might be interesting to include the interaction of distant parts of the chain in the model. Simulating the two-chains interaction will be the subject of the forthcoming study. Furthermore, studies of the HA chain in mixed water-organic solvents might be another interesting perspective of this project.

CRediT authorship contribution statement

Eva Kutálková: Conceptualization, Formal analysis, Investigation, Methodology, Resources, Software, Validation, Visualization, Writing - original draft, Writing - review & editing. **Josef Hrnčiřík:** Conceptualization, Formal analysis, Methodology, Validation, Writing - original draft, Writing - review & editing. **Roman Witasek:** Formal analysis, Investigation, Methodology, Software, Validation, Visualization. **Marek Ingr:** Conceptualization, Formal analysis, Funding acquisition, Investigation, Methodology, Project administration, Resources, Software, Supervision, Validation, Writing - original draft, Writing - review & editing.

Acknowledgment

Access to computing and storage facilities owned by parties and projects contributing to the National Grid Infrastructure MetaCentrum provided under the program "Projects of Large Research, Development, and Innovations Infrastructures" (CESNET LM2015042), is greatly appreciated.

This work was supported by The Ministry of Education, Youth and Sports from the Large Infrastructures for Research, Experimental Development and Innovations project „IT4Innovations National Supercomputing Center – LM2015070“.

Funding

This contribution was supported by Internal Funding Agency of Tomas Bata University in Zlin, projects IGA/FT/2016/011, IGA/FT/2017/009 and IGA/FT/2018/010.

MI has been supported by Grant Agency of the Czech Republic, Grant No. P208-12-G016 (Center of Excellence).

Appendix A. Supplementary data

Supplementary material related to this article can be found, in the online version, at doi:https://doi.org/10.1016/j.carbpol.2020.115919.

References

Almond, A. (2018). Multiscale modeling of glycosaminoglycan structure and dynamics: current methods and challenges. *Current Opinion in Structural Biology, 50*, 58–64. https://doi.org/10.1016/j.sbi.2017.11.008.

Almond, A., DeAngelis, P. L., & Blundell, C. D. (2005). Dynamics of hyaluronan oligosaccharides revealed by 15N relaxation. *Journal of the American Chemical Society, 127*(4), 1086–1087. https://doi.org/10.1021/ja043526i.

Almond, A., Deangelis, P. L., & Blundell, C. D. (2006). Hyaluronan: the local solution conformation determined by NMR and computer modeling is close to a contracted left-handed 4-fold helix. *Journal of Molecular Biology, 358*(5), 1256–1269. https://doi.org/10.1016/j.jmb.2006.02.077.

Bełdowski, P., Mazurkiewicz, A., Topoliński, T., & Małek, T. (2019). Hydrogen and water bonding between glycosaminoglycans and phospholipids in the synovial fluid: Molecular dynamics study. *Materials, 12*(13), 2060. https://doi.org/10.3390/ma12132060.

Benoit, H., & Doty, P. (1953). Light scattering from non-gaussian chains. *The Journal of Physical Chemistry, 57*(9), 958–963. https://doi.org/10.1021/j150510a025.

Blundell, C. D., DeAngelis, P. L., Day, A. J., & Almond, A. (2004). Use of 15N-NMR to resolve molecular details in isotopically-enriched carbohydrates: sequence-specific observations in hyaluronan oligomers up to decasaccharides. *Glycobiology, 14*(11), 999–1009. https://doi.org/10.1093/glycob/cwh117.

Buhler, E., & Boué, F. (2004). Chain persistence length and structure in hyaluronan solutions: Ionic strength dependence for a model semirigid polyelectrolyte. *Macromolecules, 37*(4), 1600–1610. https://doi.org/10.1021/ma0215520.

Donati, A., Magnani, A., Bonechi, C., Barbucci, R., & Rossi, C. (2001). Solution structure of hyaluronic acid oligomers by experimental and theoretical NMR, and molecular dynamics simulation. *Biopolymers, 59*(6), 434–445. https://doi.org/10.1002/1097-0282(200111)59:6<434::AID-BIP1048>3.0.CO;2-4.

Fouissac, E., Milas, M., Rinaudo, M., & Borsali, R. (1992). Influence of the ionic strength on the dimensions of sodium hyaluronate. *Macromolecules, 25*(21), 5613–5617. https://doi.org/10.1021/ma00047a009.

Furlan, S., La Penna, G., Perico, A., & Cesàro, A. (2005). Hyaluronan chain conformation and dynamics. *Carbohydrate Research, 340*(5), 959–970. https://doi.org/10.1016/j.carres.2005.01.030.

Guvench, O., Greene, S. N., Kamath, G., Brady, J. W., Venable, R. M., Pastor, R. W., et al. (2008). Additive empirical force field for hexopyranose monosaccharides. *Journal of Computational Chemistry, 29*(15), 2543–2564. https://doi.org/10.1002/jcc.21004.

Guvench, O., Hatcher, E., Venable, R. M., Pastor, R. W., & MacKerell, A. D. (2009). CHARMM Additive All-Atom Force Field for Glycosidic Linkages between Hexopyranoses. *Journal of Chemical Theory and Computation, 5*(9), 2353–2370. https://doi.org/10.1021/ct900242e.

Hamer, W. J., & Wu, Y. (1972). Osmotic coefficients and mean activity coefficients of uni-univalent electrolytes in water at 25°C. *Journal of Physical and Chemical Reference Data, 1*(4), 1047–1100. https://doi.org/10.1063/1.3253108.

Hayashi, K., Tsutsumi, K., Nakajima, F., Norisuye, T., & Teramoto, A. (1995). Chain-stiffness and excluded-volume effects in solutions of sodium hyaluronate at high ionic strength. *Macromolecules, 28*(11), 3824–3830. https://doi.org/10.1021/ma00115a012.

Holmbeck, S. M., Petillo, P. A., & Lerner, L. E. (1994). The solution conformation of hyaluronan: a combined NMR and molecular dynamics study. *Biochemistry, 33*(47), 14246–14255.

Humphrey, W., Dalke, A., & Schulten, K. (1996). VMD: Visual molecular dynamics. *Journal of Molecular Graphics, 14*(1), 33–38 27–28.

Ingr, M., Kutálková, E., & Hrnčiřík, J. (2017). Hyaluronan random coils in electrolyte solutions-a molecular dynamics study. *Carbohydrate Polymers, 170*, 289–295. https://doi.org/10.1016/j.carbpol.2017.04.054.

Jordan, J. H., Gibb, C. L. D., Wishard, A., Pham, T., & Gibb, B. C. (2018). Ion–hydrocarbon and/or ion–ion interactions: direct and reverse hofmeister effects in a synthetic host. *Journal of the American Chemical Society, 140*(11), 4092–4099. https://doi.org/10.1021/jacs.8b00196.

Kratky, O., & Porod, G. (1949). Rontgenuntersuchung Geloster Fadenmolekule. *Recueil Des Travaux Chimiques Des Pays-Bas-Journal of the Royal Netherlands Chemical Society, 68*(12), 1106–1122.

Mendichi, R., Soltés, L., & Giacometti Schieroni, A. (2003). Evaluation of radius of gyration and intrinsic viscosity molar mass dependence and stiffness of hyaluronan. *Biomacromolecules, 4*(6), 1805–1810. https://doi.org/10.1021/bm0342178.

Musilová, L., Kašpárková, V., Mráček, A., Minařík, A., & Minařík, M. (2019). The behaviour of hyaluronan solutions in the presence of Hofmeister ions: A light scattering, viscometry and surface tension study. *Carbohydrate Polymers, 212*, 395–402. https://doi.org/10.1016/j.carbpol.2019.02.032.

Nagarajan, B., Sankaranarayanan, N. V., & Desai, U. R. (2019). Perspective on computational simulations of glycosaminoglycans. *Wiley Interdisciplinary Reviews-Computational Molecular Science, 9*(2), e1388. https://doi.org/10.1002/wcms.1388.

Payne, W. M., Svechkarev, D., Kyrychenko, A., & Mohs, A. M. (2018). The role of hydrophobic modification on hyaluronic acid dynamics and self-assembly. *Carbohydrate Polymers, 182*, 132–141. https://doi.org/10.1016/j.carbpol.2017.10.054.

Phillips, J. C., Braun, R., Wang, W., Gumbart, J., Tajkhorshid, E., Villa, E., et al. (2005). Scalable molecular dynamics with NAMD. *Journal of Computational Chemistry, 26*(16), 1781–1802. https://doi.org/10.1002/jcc.20289.

Pogany, P., & Kovacs, A. (2010). Theoretical study of hyaluronan oligosaccharides. *Structural Chemistry, 21*(6), 1185–1194. https://doi.org/10.1007/s11224-010-9658-y.

Pomin, V. H. (2014). NMR-based dynamics of free glycosaminoglycans in solution. *Analyst, 139*(15), 3656–3665. https://doi.org/10.1039/C4AN00531G.

Salis, A., Cugia, F., Parsons, D. F., Ninham, B. W., & Monduzzi, M. (2012). Hofmeister series reversal for lysozyme by change in pH and salt concentration: insights from electrophoretic mobility measurements. *Journal of the Chemical Society Faraday Transactions, 14*(13), 4343–4346. https://doi.org/10.1039/C2CP40150A.

Siódmiak, J., Bełdowski, P., Augé, W. K., Ledziński, D., Śmigiel, S., & Gadomski, A. (2017). Molecular dynamic analysis of hyaluronic acid and phospholipid interaction in tribological surgical adjuvant design for osteoarthritis. *Molecules (Basel, Switzerland), 22*(9), https://doi.org/10.3390/molecules22091436.

Smith, P., Ziolek, R. M., Gazzarrini, E., Owen, D. M., & Lorenz, C. D. (2019). On the interaction of hyaluronic acid with synovial fluid lipid membranes. *Journal of the Chemical Society Faraday Transactions, 21*(19), 9845–9857. https://doi.org/10.1039/C9CP01532A.

Zhang, Y., & Cremer, P. S. (2009). The inverse and direct Hofmeister series for lysozyme. *Proceedings of the National Academy of Sciences, 106*(36), 15249–15253. https://doi.org/10.1073/pnas.0907616106.